4 Characterization of macrostresses

R. A. Winholtz

4.1 Macrostresses

Residual macrostresses are what have classically been thought of as residual stresses. Macrostresses arise in considering a macroscopic view where the material is considered homogeneous. They are the stresses that are revealed by dissection methods of residual stress measurement such as hole drilling or sectioning. Residual macrostresses are well known to affect material properties. They can be beneficial or detrimental to a material's performance. Fatigue resistance, for example, can be improved or reduced by tensile or compressive stresses, respectively, near the surface. Macrostresses also inhibit the ability to maintain dimensional control of components during manufacturing operations because, as stressed material is removed, stresses redistribute and the remaining material distorts.

For these reasons, the characterization of residual stresses is an important engineering consideration. Measurement of residual stresses is important both for directly knowing the stresses produced by various processes and for validating models of residual stress-producing processes. Diffraction methods are attractive for measuring residual stresses because they are nondestructive, precise, able to measure stresses both near the surface and in the interior of materials, and able to give the entire three-dimensional (3D) stress tensor.

4.2 Measurement of stresses with diffraction

Diffraction can be used to precisely measure a lattice spacing utilizing Bragg's law:

$$\lambda = 2d \sin\theta \tag{1}$$

Here, λ is the wavelength of the radiation used, θ is one-half the scattering angle, and d is the average interplanar spacing for a given reflection in a crystalline material. In a stressed material, the lattice spacing can be used as a strain gauge, giving a measure of linear strain in the direction of the diffraction vector. If d_0 and θ_0 are the lattice spacing and the corresponding Bragg angle measured for the stress-free material, the strain can be computed as

$$\varepsilon = \frac{d - d_0}{d_0} = \frac{\sin\theta_0}{\sin\theta} - 1 \tag{2}$$

The state of strain at some location in a material is a second-order tensor quantity represented by shear and normal components referenced to a given coordinate system. We can determine the state of strain in a material using diffraction by measuring the linear or normal strain in a number of directions and utilizing the rules specifying how the components of a second-order tensor transform with direction. Having determined the strain components, the stress components are then computed using Hooke's law.

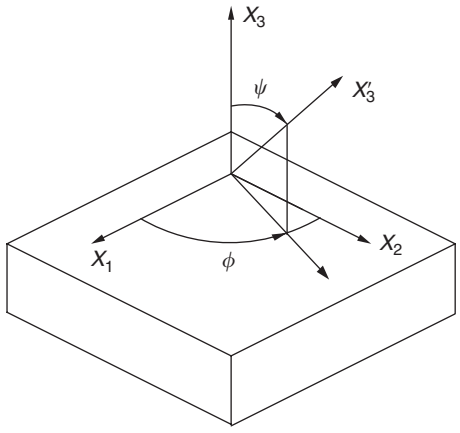

Figure 4.1 Coordinate systems used to measure stresses with diffraction. The X_i coordinate axes are the sample coordinate system. Oriented by the angles ϕ and ψ with the sample coordinate system is the X_3' axis of the laboratory coordinate system.

First, we set up two coordinate systems illustrated in Figure 4.1. The X_i coordinate system is the sample coordinate system. We wish to determine the strain and stress components in this sample coordinate system. Although we are free to attach this coordinate system to the material in any way we desire, the geometry of the component will often suggest a natural set of sample coordinates. For near surface stress measurements using X-rays it is customary to place the X_3 axis normal to the surface. The X_3' coordinate axis is in the laboratory system, which is the reference frame for making the diffraction measurements. The X_3' coordinate axis is oriented with respect to the sample coordinate axes by the angles ϕ and ψ as shown in Figure 4.1. By orienting the specimen with respect to the incident and diffracted beams such that the diffraction vector is along the X_3' axis, we can measure the strain in this direction, designated $\varepsilon_{\phi\psi}$. A diffraction peak is recorded and its Bragg angle precisely determined. The strain is then determined using equation (2).

Next, we relate the strain measured in the laboratory coordinate system to the unknown strain components in the sample coordinate system. Strain components transform according to the relation [1]

$$\varepsilon'_{ij} = \alpha_{ik}\alpha_{jl}\varepsilon_{kl} \tag{3}$$

where α_{ij} are the direction cosines between the laboratory and sample coordinate systems defined as

$$\alpha_{ij} = \cos(X'_i, X_j) \tag{4}$$

In equation (3) and in what follows, repeated indices imply summation. The direction cosines between the laboratory and sample coordinate systems are

$$\begin{aligned} \alpha_{31} &= \cos\phi \sin\psi \\ \alpha_{32} &= \sin\phi \sin\psi \\ \alpha_{33} &= \cos\psi \end{aligned} \tag{5}$$

Substituting these into equation (3) we obtain

$$\varepsilon_{\phi\psi} = \frac{d_{\phi\psi} - d_0}{d_0} = \varepsilon_{11}\cos^2\phi\sin^2\psi + \varepsilon_{22}\sin^2\phi\sin^2\psi + \varepsilon_{33}\cos^2\psi + \varepsilon_{12}\sin 2\phi\sin^2\psi + \varepsilon_{13}\cos\phi\sin 2\psi + \varepsilon_{23}\sin\phi\sin 2\psi \tag{6}$$

This equation relates the quantities we measure with diffraction, $d_{\phi\psi}$ and d_0, to the unknown quantities we want to determine, the components of strain in the material ε_{ij}. There are six unknown strain components, thus we must measure at least six strains, $\varepsilon_{\phi\psi}$, at ϕ and ψ angles that do not form a singular set of equations. A least-squares solution of equation (6) can be obtained when more than six diffraction strain measurements are made [2]. This is good practice, minimizing the effects of a single bad measurement and allowing an assessment of the quality of the least-squares fit to the experimental data.

Having obtained the strain tensor, the stress tensor is then obtained from Hooke's law

$$\sigma_{ij} = \frac{1}{(1/2)S_2}\left[\varepsilon_{ij} - \delta_{ij}\frac{S_1}{(1/2)S_2 + 3S_1}\varepsilon_{ii}\right] \tag{7}$$

where S_1 and $(1/2)S_2$ are the diffraction elastic constants [3, 4].

4.3 Least-squares determination of the strain tensor

To facilitate a matrix formulation for computer solution we introduce the following definitions [2]:

$$\begin{aligned}
\varepsilon_1 &= \varepsilon_{11} & f_1(\phi,\psi) &= \cos^2\phi\sin^2\psi \\
\varepsilon_2 &= \varepsilon_{22} & f_2(\phi,\psi) &= \sin^2\phi\sin^2\psi \\
\varepsilon_3 &= \varepsilon_{33} & f_3(\phi,\psi) &= \cos^2\psi \\
\varepsilon_4 &= \varepsilon_{12} & f_4(\phi,\psi) &= \sin 2\phi\sin^2\psi \\
\varepsilon_5 &= \varepsilon_{13} & f_5(\phi,\psi) &= \cos\phi\sin 2\psi \\
\varepsilon_6 &= \varepsilon_{23} & f_6(\phi,\psi) &= \sin\phi\sin 2\psi
\end{aligned} \tag{8}$$

We may then rewrite equation (6) as

$$\varepsilon_{\phi\psi} = \varepsilon' = \sum_{j=1}^{6}\varepsilon_j f_j(\phi,\psi) \tag{9}$$

We define the weighted sum of squared error χ^2 as

$$\chi^2 = \sum_{i=1}^{n}\frac{(\varepsilon_{\text{obs}} - \varepsilon_{\text{calc}})^2}{\text{var}(\varepsilon_i')} = \sum_{i=1}^{n}\frac{1}{\text{var}(\varepsilon_i')}\left(\varepsilon_i' - \sum_{j=1}^{n}\varepsilon_j f_j(\phi_i,\psi_i)\right)^2 \tag{10}$$

Here, the number of strain measurements collected is n and $\text{var}(\varepsilon_i')$ is an estimate of the variance (squared standard deviation) or uncertainty in the ith strain measurement. The values of $\text{var}(\varepsilon_i')$ are found by propagating the uncertainty in the peak locations to the strains.

Each $\text{var}(\varepsilon_i')$ provides a weighting factor on each strain measurement's contribution to χ^2 so that those with a smaller standard deviation make a larger contribution. We want to find the values of the ε_j that minimize χ^2. A minimum in χ^2 exists when its partial derivative with respect to each ε_j equals zero. Taking the partial derivatives results in the set of equations

$$\frac{\partial \chi^2}{\partial \varepsilon_j} = \sum_{i=1}^{n} \left[\left(\sum_{k=1}^{6} \varepsilon_k f_k(\phi_i, \psi_i) \right) - \varepsilon_i' \right] \frac{f_j(\phi_i, \psi_i)}{\text{var}(\varepsilon_i')} = 0 \tag{11}$$

Forming the matrix $\mathbf{B}$ and the vector $\mathbf{E}$ with elements

$$\begin{aligned} B_{jk} &= \sum_{i=1}^{n} f_j(\phi_i, \psi_i) f_k(\phi_i, \psi_i)/\text{var}(\varepsilon_i') \\ E_j &= \sum_{i=1}^{n} \varepsilon_i' f_j(\phi_i, \psi_i)/\text{var}(\varepsilon_i') \end{aligned} \tag{12}$$

gives the matrix equation

$$\mathbf{B\varepsilon} = \mathbf{E} \tag{13}$$

This is the set of normal equations for the least-squares solution. It can be solved by matrix inversion or other methods [5] for the strain components ε_j,

$$\boldsymbol{\varepsilon} = \mathbf{B}^{-1}\mathbf{E} \tag{14}$$

4.4 The $\sin^2 \psi$ method

The $\sin^2 \psi$ method is the traditional method for measuring near surface stresses with X-rays [3, 4]. There is a wealth of experience in interpreting diffraction stress data in this form and much of the anomalous behaviors seen have been studied and interpreted in this context. The $\sin^2 \psi$ method utilizes the fact that the d-spacing between any two principal directions will be linear with the square of the sine of the angle between them. This method has its origins in graphical solution methods before widespread computer usage and is still very useful for visualizing and understanding data.

We first substitute Hooke's law, equation (7), into the fundamental diffraction strain relation, equation (6), and use $\cos^2\psi = 1 - \sin^2\psi$ to obtain

$$\begin{aligned} \varepsilon_{\phi\psi} = \frac{d_{\phi\psi} - d_0}{d_0} &= (1/2)S_2(\sigma_{11}\cos^2\phi + \sigma_{12}\sin 2\phi + \sigma_{22}\sin^2\phi - \sigma_{33})\sin^2\psi \\ &\quad + (1/2)S_2\sigma_{33} + S_1(\sigma_{11} + \sigma_{22} + \sigma_{33}) \\ &\quad + (1/2)S_2(\sigma_{13}\cos\phi + \sigma_{23}\sin\phi)\sin 2\psi \end{aligned} \tag{15}$$

In the near-surface region, the stresses σ_{i3} cannot exist as macrostresses [3, 6]. In many instances microstresses will be zero and these terms will vanish. We define the stress

$$\sigma_\phi = \sigma_{11}\cos^2\phi + \sigma_{12}\sin 2\phi + \sigma_{22}\sin^2\phi \tag{16}$$

as the stress component along the ϕ direction in the sample surface. Equation (15) then becomes

$$\varepsilon_{\phi\psi} = \frac{d_{\phi\psi} - d_0}{d_0} = (1/2)S_2\sigma_\phi \sin^2\psi + S_1(\sigma_{11} + \sigma_{22}) \tag{17}$$

This equation shows that $\varepsilon_{\phi\psi}$ or $d_{\phi\psi}$ is linear with $\sin^2\psi$ for a constant ϕ. The slope of the measured d-spacings will be proportional to the stress σ_ϕ. Because we have a biaxial stress state, d_0 is just a multiplier in the slope and a precise value is not necessary to determine the stress σ_ϕ. Any uncertainty in d_0, easily determinable to a fraction of a percent, is reflected to the same proportion in the uncertainty in stress and is generally negligible in comparison to other uncertainties.

The stresses σ_{i3} can be present in the near-surface region as microstresses or they may be present in the interior or materials and measurable with neutrons or high-energy X-rays. The $\sin^2\psi$ method is also applicable for these situations where the stresses σ_{i3} are present. First, consider σ_{33} being present. Examining equations (15) and (16), we see that the slope of d-spacing (or strain $\varepsilon_{\phi\psi}$) versus $\sin^2\psi$ is proportional to the difference between stresses

$$\text{slope} \propto \sigma_\phi - \sigma_{33} \tag{18}$$

In order to determine the values of these stresses independently, we must also utilize the intercept of d versus $\sin^2\psi$. To determine the intercept with sufficient precision we must know the value of d_0 better than the precision of the strains being measured. This will be illustrated further in Section 4.8.

Now consider the case where the shear stresses σ_{13} and σ_{23} are present in the diffracting volume. Equation (15) shows that these two stress components will cause the d-spacing to be nonlinear with respect to $\sin^2\psi$. For measurements at a constant ϕ, the $\sin 2\psi$ term will have the same magnitude but opposite sign for positive and negative ψ value. The d-spacing will show two branches for positive and negative ψ forming an ellipse as shown in Figure 4.2.

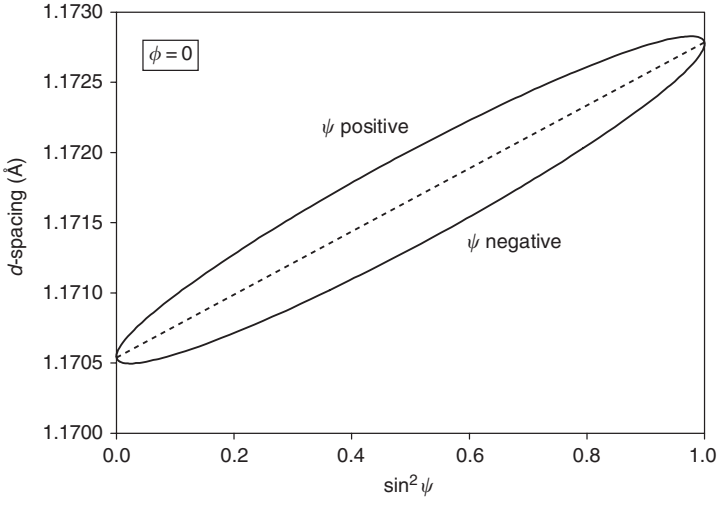

Figure 4.2 Illustration of ψ-splitting in a d versus $\sin^2\psi$ plot. The d-spacings are calculated from equation (6) with a shear strain ε_{13} present.

This is known as ψ-splitting. For near-surface measurements one cannot typically get to $\sin^2\psi = 1.0$ ($\psi = 90°$) and the ellipse does not close back up. For bulk measurements with penetrating radiations, however, one can measure out to $\psi = \pm 90°$ where one is measuring the same strain in opposite directions. From the centerline of the ellipse, or the average value between positive and negative ψ branches, one can get the normal stress components from the slope and intercept as previously done. This works because the averaging removes the shear components σ_{13} or σ_{23} since they have opposing contributions for the positive and negative ψ branches. The height of the ellipse can then be used to obtain the shear stress values. The deviation of d-spacing from the centerline versus $\sin 2\psi$ will have a slope proportional to the shear stress. By looking at the deviation from the centerline of the ellipse we have removed to the contributions of the normal stress components.

Analyzing data in this fashion is known as the Dölle–Hauk method [4, 7, 8]. It should be noted that the least-squares approach will handle all the stress components automatically and can give improved precision [2] but does not preclude one from plotting the d-spacings at constant ϕ sections versus $\sin^2\psi$ to inspect it for anomalies.

4.5 Determining the stress-free lattice spacing d_0

For the measurement of triaxial stress states a precise value of the stress-free lattice spacing d_0 is necessary to obtain the stresses and strains. Determining this value can be problematic [9]. One must measure a stress-free version of the material with the same experimental configuration used to measure the stressed material in order to remove any systematic 2θ shifts present. While such deviations from the absolute d-spacings measured can be made small, strains are also quite small and one should not try to rely on published values of lattice parameters. Another reason published values cannot be used is that, for many materials of engineering interest, the lattice parameter will vary with thermo-mechanical treatment. This can occur due to the formation of precipitates that can change the composition of phases. Differences in the stacking fault density can also change the stress-free value, in some materials [9, 10]. Another problem is that the value of d_0 can vary with location in a material due to differences in thermo-mechanical treatment with position (which may have produced the residual stresses).

Several methods can be used to determine the stress-free value at a given location in the material. First, a stress-free powder can be measured. A powder will be genuinely stress free. Any internal stresses in a powder particle must balance with each other giving an average stress of zero in all the particles. Care must be taken in using this method to be sure that the powder has the stress-free value of interest. The powder may not have the same thermo-mechanical treatment as the stressed material and hence may be unusable. This presents a difficulty because the method to produce a powder must be inherently different than the method used to produce the component of interest. For example, precipitation hardening aluminum alloys will have a different stress-free lattice spacing when used as the matrix for a composite than when they are a bulk alloy even with the same heat treatments. The presence of the reinforcing phase changes the precipitation kinetics, changing the stress-free lattice spacing [11–13]. Thus, filings from a bulk alloy may be unsuitable for measuring d_0.

Second, one may go to an unstressed region of a component to measure the stress-free lattice spacing. This method works nicely when appropriate because it does not involve any extra experimental set up. Here, one must be concerned that there is truly an unstressed region in the component. One must also be sure that d_0 is independent of position in the material. For a multiphase material, this method gives a macrostress-free lattice spacing that may still

contain effects from microstresses. If one wants to determine only the macrostresses and the microstresses do not vary with position, this is appropriate.

Another method is to take an identical companion component and cut it up into small stress-free coupons to measure [14]. One must ensure that the cutting operation relaxes the residual macrostresses without introducing new residual stresses. Metals can often be electro-discharge machined to produce the coupons. Concerns in using this method include being sure that the coupons are cut to a small enough size so that macrostresses are substantially relieved and that the d_0 variations are captured sufficiently. It is also a disadvantage that a second component must be sacrificed, giving up the nondestructive nature of the diffraction stress measurement. This method will again give only macrostress-free values.

If one is confident that it does not vary with location in the component, equilibrium can be used to determine d_0. Any component of stress must integrate to zero over a cross-section of the component

$$\int_A \sigma_{ij} \mathrm{d}A = 0 \tag{19}$$

One may iteratively try d_0 values until equation (19) is satisfied and then use this value.

Finally, if none of these methods is amenable, one may use an inaccurate value of d_0 and report the estimated error. It will be shown in Section 4.8 that an inaccurate value of d_0 leads to an error in the hydrostatic part of the stress. In many instances accurate values of the deviatoric stresses may provide the information necessary for the problem at hand.

4.6 Assuming principal directions

For subsurface measurements of stress with penetrating radiations, there is an incentive to save time in making measurements because intensities are often quite low, due to absorption by the sample, and source accessibility can be limited and expensive. If one knows the directions of the principal strains, time can be saved by measuring only in the three principal directions instead of trying to measure the general state of strain represented by equation (6). Geometry or loading can often suggest the principal directions.

Ignoring any shear stresses that are present and measuring three perpendicular strains will not lead to any error in the three normal components of stress. From equation (6) one can see that the shear strain components do not make any contribution to the measured strains along the sample coordinate axes, that is, for (ϕ, ψ) equal to $(0, 90^\circ)$, $(90^\circ, 90^\circ)$ and $(0, 0)$. The form of Hooke's law used for polycrystalline materials, equation (7), has no coupling between shear and normal stresses and strains. This means that the three normal components of stress can be determined whether or not they are the principal directions [15]. This can be useful in simplifying measurements made to compare to a finite element computation or analytic model where components of stress are sufficient. One should be careful in neglecting the shear stress components, however. The normal stress components may not accurately reflect the complete stress state of the material. The principal stresses may be much larger, limited only by the strength of the material.

The stress equilibrium relation $\sigma_{ij,j} = 0$ can be helpful in examining assumptions about the principal stress directions [16]. If one has stress data obtained from measuring strains in three orthogonal directions in a sample, this relation may be used to prove they are not the principal directions. If any normal component of stress σ_{ii} varies with the direction X_i then the equilibrium relation tells us there must be gradients in the shear stresses as well. For

example, if we see that σ_{11} has a gradient in the X_1 direction we may use

$$\frac{\partial \sigma_{11}}{\partial X_1} + \frac{\partial \sigma_{12}}{\partial X_2} + \frac{\partial \sigma_{13}}{\partial X_3} = 0 \tag{20}$$

to see that there are gradients in the shear stresses in the X_2–X_3 plane. Since the shear stresses are varying in this plane, they cannot be zero everywhere in this plane. If there are shear stress components present, the normal stress components are not the principal stresses. While the equilibrium relation may confirm that a set of stress measurements are not the principal stresses, it cannot be used to prove that they are the principal directions. This relation only deals with gradients so a constant shear stress can be present if σ_{ii} does not vary with X_i.

4.7 Error analysis

An error analysis of diffraction stress measurements is important for a number of reasons. First, elastic strains in crystalline materials are very small and it is easy to have the uncertainties in the measurements exceed the size of the strains due to the stresses. One needs an estimate of the errors to ensure that the results are meaningful. Second, one can use an error analysis to examine the feasibility of a proposed measurement. Time considerations may be important here as well, as higher precision measurements usually take more counting time. For example, after a preliminary error analysis one might conclude that a proposed set of measurements can achieve a desired level of uncertainty but the time necessary far exceeds that reasonably available. One should generally use an error analysis to design an experiment to achieve a given level of uncertainty in the final results. Third, error analysis can be used to optimize a measurement strategy. One will want to examine absorption path lengths for various potential measurement orientations to choose the ϕ and ψ values used to make the measurements. One wants to minimize the measurement uncertainties for a given amount of measurement time. Conversely, one may want to minimize the measurement time necessary to achieve a given level of measurement uncertainty. Access to neutron and synchrotron sources can be expensive and limited so the best use of the available time should be used.

For a quantity x observed repeatedly n times, the variance is defined as

$$\mathrm{var}(x) = \frac{\sum_{i=1}^{n} (x_i - \bar{x})^2}{n-1} \tag{21}$$

where $\bar{x}$ is the average of the observations.

The objective of the error analysis is to identify and quantify the sources of error in the measurements and propagate them into the final results. Measurement uncertainties or errors are propagated as follows. Consider a result y calculated from several measured variables x_i

$$y = f(x_1, x_2, \ldots) \tag{22}$$

For random errors in the measured variables, the variance in y as a function of the variances in x_i is given by [17]

$$\mathrm{var}(y) = \left(\frac{\partial y}{\partial x_1}\right)^2 \mathrm{var}(x_1) + \left(\frac{\partial y}{\partial x_2}\right)^2 \mathrm{var}(x_2) + \cdots + 2\left(\frac{\partial y}{\partial x_1}\right)\left(\frac{\partial y}{\partial x_2}\right) \mathrm{cov}(x_1, x_2) + \cdots \tag{23}$$

The error in y is then often reported as one standard deviation in y

$$\text{Error in } y = \text{std}(y) = \sqrt{\text{var}(y)} \tag{24}$$

For diffraction stress measurements, the primary source of uncertainty in the stress and strain tensors is the uncertainties in the locations of the diffraction peaks. These will be both random and systematic. Random errors in the location of diffraction peaks include the counting statistics of measuring intensities with a detector, electronic noise and stability in the detector system, temperature fluctuations during the measurements, and many others. In many cases, for a properly working system, the counting statistics can dominate the random errors. We would like to be able to estimate the random errors from a single observation of a diffraction peak rather than observing it often enough to see the actual variation given by equation (21). The random error in the peak location is usually estimated by the fitting program that is used to determine the peak location. This will give an estimate of the variation expected due to counting statistics if the peak were observed many times.

Systematic errors include diffractometer misalignment, absorption effects and geometrical effects associated with a gauge volume. There can also be systematic irregularities in the specimen leading to measurement errors such as an unsuitable stress-free standard or the stress-free lattice spacing varying with location in the material. It is hoped that care is taken and that the systematic errors are removed from the measurements or at least understood and the data corrected for them. Systematic errors that are constant in both the measurement of $d_{\phi\psi}$ and d_0, such as an error in the radiation wavelength or a 2θ offset, will cancel each other in equation (2) resulting in no errors in the strain measurements.

The total variance in peak location can be estimated as the sum of the variance due to counting statistics and the variance due to other sources

$$\text{var}(2\theta_t) = \text{var}(2\theta_{cs}) + \text{var}(2\theta_{os}) \tag{25}$$

The variance due to counting statistics can be controlled by the number of counts collected in the diffraction peak. Generally, one must count four times longer to reduce the standard deviation by one half. One may estimate the variance due to other sources for a particular instrument by repeatedly observing a diffraction peak with long count times to give as equation (21) and then equation (25) is used to estimate $\text{var}(2\theta_{os})$.

To get the error in each strain measurement we apply equation (23) to equation (2) and obtain

$$\text{var}(\varepsilon_{\phi\psi}) = \text{var}(\varepsilon_i') = \left(\frac{\sin\theta_0 \cos\theta}{\sin^2\theta}\right)^2 \text{var}(\theta) + \left(\frac{\cos\theta_0}{\sin\theta}\right)^2 \text{var}(\theta_0) \tag{26}$$

or

$$\text{var}(\varepsilon_{\phi\psi}) \cong \cot\theta \frac{1}{4}[\text{var}(2\theta) + \text{var}(2\theta_0)] \left(\frac{180}{\pi}\right)^2 \tag{27}$$

which relates the variance in a strain to the variances in the measured Bragg peak locations. In equation (27) we have switched from θ to 2θ, the experimentally determined variable, and added a conversion from radians to degrees because peak positions are generally determined in degrees.

The errors in each measured strain are then propagated through the least-squares solution to the strain components in the sample coordinate system

$$\mathrm{var}(\varepsilon_k) = \sum_{i=1}^{n} \left(\frac{\partial \varepsilon_k}{\partial \varepsilon_i'} \right)^2 \mathrm{var}(\varepsilon_i') \tag{28}$$

This result assumes that the individual strain measurements, ε_i', are independent so that the covariance terms are zero. It can be shown that applying equation (28) to equation (14) gives the result [5]

$$\mathrm{var}(\varepsilon_k) = [\mathbf{B}]_{kk}^{-1} \tag{29}$$

That is, the diagonal elements of the inverse of the matrix **B** are the variances of the corresponding strain components. Furthermore, $\mathbf{B}^{-1}$ is the covariance matrix and the off-diagonal elements give the covariance between corresponding strain components [5]

$$\mathrm{cov}(\varepsilon_i, \varepsilon_j) = [\mathbf{B}]_{ij}^{-1} \tag{30}$$

Care must be exercised in including the variance in the stress-free lattice spacing in equation (27). If a number of measurements of strain all use the same d_0 (or θ_0) value, they are not random and independent of each other but are perfectly correlated [18]. This makes the use of equation (28) invalid. Handling the error in d_0 in this case is shown in Section 4.8. If a separate value of d_0 is measured for each $\varepsilon_{\phi\psi}$, then the random errors are uncorrelated and its inclusion in equation (27) is the correct way to handle the error.

After obtaining the errors in the strain components, it is propagated into the stress components by applying equation (23) to equation (7) resulting in

$$\begin{aligned}
\mathrm{var}(\sigma_{11}) = {} & \left[\frac{1}{(1/2)S_2} - \frac{S_1}{(1/2)S_2((1/2)S_2 + 3S_1)} \right]^2 \mathrm{var}(\varepsilon_{11}) \\
& + \left[\frac{S_1}{(1/2)S_2((1/2)S_2 + 3S_1)} \right]^2 [\mathrm{var}(\varepsilon_{22}) + \mathrm{var}(\varepsilon_{33})] \\
& + 2 \left[\frac{1}{(1/2)S_2} - \frac{S_1}{(1/2)S_2((1/2)S_2 + 3S_1)} \right] \left[\frac{S_1}{(1/2)S_2((1/2)S_2 + 3S_1)} \right] \\
& \times [\mathrm{cov}(\varepsilon_{11}, \varepsilon_{22}) + \mathrm{cov}(\varepsilon_{11}, \varepsilon_{33})] \\
& + 2 \left[\frac{S_1}{(1/2)S_2((1/2)S_2 + 3S_1)} \right]^2 \mathrm{cov}(\varepsilon_{22}, \varepsilon_{33})
\end{aligned} \tag{31}$$

for the normal stress σ_{11}, the variances for σ_{22} and σ_{33} being similar in form. For the shear stress components we obtain

$$\mathrm{var}(\sigma_{ij}) = \left[\frac{1}{(1/2)S_2} \right]^2 \mathrm{var}(\varepsilon_{ij}); \quad i \neq j \tag{32}$$

Covariance terms exist in equation (31) because the normal stresses are coupled to all three normal strains, while they are absent in equation (32) because each shear stress component depends only on its corresponding shear strain.

If normal stress components are determined by measuring strain in three orthogonal directions, equation (31) is used to estimate the errors in the stress components by setting the strain covariance terms equal to zero. They are zero because the orthogonal strain measurements are independent of each other.

The relations for errors in diffraction stress measurements are also useful in estimating the time necessary for a set of experiments and their feasibility. Preliminary measurements of a sample of the material to be studied can be scaled to estimate the time necessary to achieve the desired precision. Such planning will help prevent unacceptably high errors in a set of measurements or running out of available time.

The time necessary to achieve a given error level in a set of measurements can be estimated from a preliminary measurement of a diffraction peak. The desired level of error in the stress and strain tensors is used to compute the necessary errors in the peak positions using the relations above. The time necessary to measure each diffraction peak for a series of measurements is then estimated from a preliminary measurement using the relation [19]

$$\mathrm{var}(2\theta_i) = \mathrm{var}(2\theta_0)\left(\frac{t_0}{t_i}\right)\exp[\mu(l_i - l_0)] \tag{33}$$

Here t is the time taken to collect a diffraction peak with a variance $\mathrm{var}(2\theta)$ through a beam path length through the sample of l. The subscript '0' indicates these quantities for a preliminary measurement and the subscript 'i' designates these quantities for each of the diffraction peaks in the planned measurements. The absorption coefficient for the material is given by μ. By summing the times necessary to achieve the necessary precision in the peak positions one can estimate the time needed. Some iteration may be necessary to find a satisfactory measurement plan.

4.8 Uncertainties in the stress-free lattice spacing d_0

For triaxial stress measurements the stress-free lattice spacing d_0 must be measured to a precision better than the precision desired in the strains. We can illustrate the role of d_0 in diffraction stress measurement by substituting hydrostatic, ε_{H}, and deviatoric, $\backprime\varepsilon_{ij}$, parts of the strain tensor into equation (6) and obtaining

$$\begin{aligned} d_{\phi\psi} = d_0 + d_0\varepsilon_{\mathrm{H}} + d_0[&\backprime\varepsilon_{11}\cos^2\phi\sin^2\psi + \backprime\varepsilon_{22}\sin^2\phi\sin^2\psi + \backprime\varepsilon_{33}\cos^2\psi \\ &+ \backprime\varepsilon_{12}\sin 2\phi\sin^2\psi + \backprime\varepsilon_{13}\cos\phi\sin 2\psi + \backprime\varepsilon_{23}\sin\phi\sin 2\psi] \end{aligned} \tag{34}$$

This equation still has only six unknown strain components on the right-hand side as the relation

$$\backprime\varepsilon_{11} + \backprime\varepsilon_{22} + \backprime\varepsilon_{33} = 0 \tag{35}$$

follows from the definition of the strain deviator. Using this, we obtain

$$\begin{aligned} d_{\phi\psi} = d_0 + d_0\varepsilon_{\mathrm{H}} + d_0[&\backprime\varepsilon_{11}(\cos^2\phi\sin^2\psi - \cos^2\psi) + \backprime\varepsilon_{22}(\sin^2\phi\sin^2\psi - \cos^2\psi) \\ &+ \backprime\varepsilon_{12}\sin 2\phi\sin^2\psi + \backprime\varepsilon_{13}\cos\phi\sin 2\psi + \backprime\varepsilon_{23}\sin\phi\sin 2\psi] \end{aligned} \tag{36}$$

By measuring $d_{\phi\psi}$ as a function of direction and utilizing equations (35) and (36), one can determine the deviatoric components of the strain since each has a different trigonometric dependence on the angles ϕ and ψ. An accurate value of d_0 is unnecessary since it is only a multiplier in each term. From the dependence of $d_{\phi\psi}$ with orientation one can also determine the constant component that does not vary with ϕ and ψ. However, the hydrostatic part of the strain cannot be determined without a precise value for d_0 because there are two constant terms in equation (36), which cannot be distinguished from each other with measurements of $d_{\phi\psi}$ [18, 20]. Thus, the precision to which d_0 is known determines the precision to which the hydrostatic strain can be known. Any error in d_0 results directly in an error in the hydrostatic component of strain and stress.

Having obtained the hydrostatic and deviatoric parts of the strain, the corresponding parts of the stress are obtained from

$$\sigma_{\mathrm{H}} = \frac{E}{(1-2\nu)}\varepsilon_{\mathrm{H}} = \frac{1}{(1/2)S_2 + 3S_1}\varepsilon_{\mathrm{H}} \tag{37}$$

$$\text{`}\sigma_{ij} = \frac{E}{1+\nu}\text{`}\varepsilon_{ij} = \frac{1}{(1/2)S_2}\text{`}\varepsilon_{ij} \tag{38}$$

The error in the hydrostatic part of the stress tensor due to d_0 is then

$$\mathrm{var}(\sigma_{\mathrm{H}}) = \left(\frac{1}{(1/2)S_2 + 3S_1}\right)^2 \left(\frac{1}{d_0}\right)^2 \mathrm{var}(d_0) \tag{39}$$

In practice, one can just fit equation (6) and perform an error analysis assuming no uncertainty in d_0. One can then use equation (39) to find the error in the hydrostatic part of the stress and add it in quadrature to the previous errors on the normal stress components.

4.9 Uncertainties in the principal stresses and directions

Having determined the components of the stress tensor one may then compute the principal stresses and directions by solving the eigenvalue problem [21]

$$\begin{bmatrix} \sigma_i - \sigma_{11} & -\sigma_{12} & -\sigma_{13} \\ -\sigma_{12} & \sigma_i - \sigma_{22} & -\sigma_{23} \\ -\sigma_{13} & -\sigma_{23} & \sigma_i - \sigma_{33} \end{bmatrix} \begin{bmatrix} \alpha_{i1} \\ \alpha_{i2} \\ \alpha_{i3} \end{bmatrix} = 0 \tag{40}$$

Three solutions for σ_i exist which are the principal stresses. The α_{ij} for each σ_i give the direction cosines describing the corresponding principal direction. Along with the principal stresses and directions, estimates of their errors should also be reported. Since equation (23) cannot be applied to the solution of equation (40), an alternate approach to estimate the errors is necessary.

A Monte Carlo approach can be used to simulate the propagation of errors through the data analysis by repeatedly generating sets of synthetic data with a random number generator and analyzing them [22]. The distribution of principal stresses and their directions are then used to estimate errors. It should be emphasized that the errors in the synthetic data sets are distributed about one particular experimental measurement and not about the true values of stress. It is assumed the distribution of errors about the true values have the same shape and variance as the distribution produced from the computer simulation and is thus useful for estimating the errors in the measurement.

To estimate the errors in the stresses with the Monte Carlo approach, we proceed as follows. Each observation of an intensity in the original data set is replaced with a new one from a random number generator. Each diffraction peak collected at an orientation of the sample will consist of the original intensities measured over a range of 2θ values. This data is fit to a function, such as a Gaussian, Lorentzian, or pseudo-Voigt, to determine the peak position. The peak fits to the original data form the basis for generating the synthetic data sets. The value of the best fit function is taken at each 2θ and then an error is added. This error is taken from a random number generated from a normal distribution with a zero mean and a standard deviation equal to the square root of the number of counts. This simulates adding counting statistics to the best fit peak function to get a synthetic data set. Figure 4.3 illustrates this process, showing the best fit Gaussian function to an original diffraction peak, a new set of synthetic data generated from this profile, and a new best fit Gaussian function to the new synthetic data. Notice that the fit to the synthetic data gives a slightly different peak position because of the new random noise added.

Once this process has been applied to all the diffraction peaks in a measurement, the new synthetic data set is analyzed in the same manner as the original data giving a stress tensor with principal stresses and directions. These values are recorded and the process repeated with a newly generated set of synthetic data. An ensemble of stress tensors and corresponding principal stresses and directions is thus generated by repeating this process. Several hundred synthetic data sets should be sufficient. The standard deviation in each stress component and principal stress can be computed from this ensemble giving an estimate of the errors in the original measurement. Errors estimated in the stress components by the Monte Carlo approach have been shown to be equivalent to those given by equations (31) and (32) [23]. The Monte Carlo method has the advantage that it can be extended to the principal stresses.

To estimate the likely errors in the principal stress directions, the ensemble of principal directions from the Monte Carlo analysis can all be plotted on an equal area projection [24]

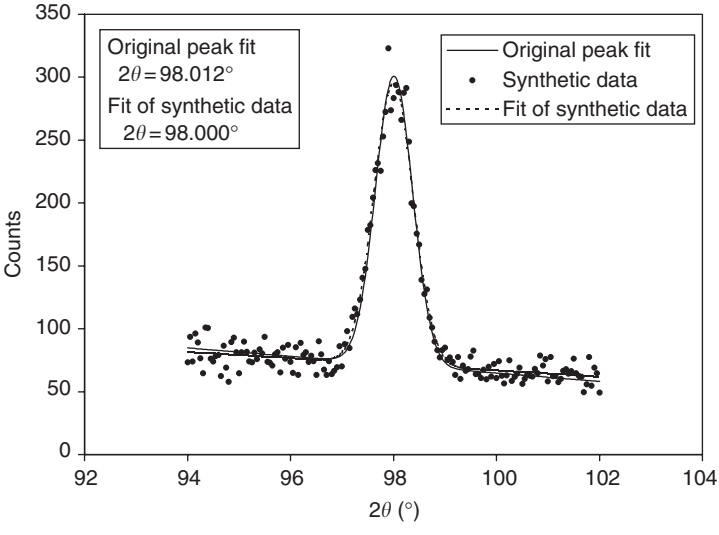

Figure 4.3 Illustration of generating a synthetic data set. The peak fit to the original data is shown along with a synthetic data set created by adding noise to the original peak fit. The best fit to the synthetic data is also shown which has a slightly different peak position.

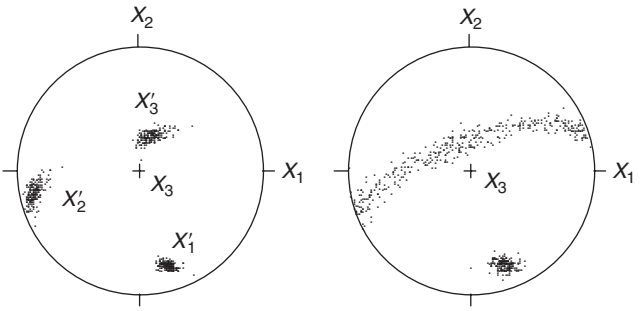

Figure 4.4 Equal area plots showing the results of a Monte Carlo calculation of the principal stress directions. These plots reveal the likely uncertainty in the principal directions.

to observe their distribution. An equal area projection is used because random directions will show up with a uniform density. Figure 4.4 shows two such plots from the same location in a weld before and after post-weld heat treatment [25]. The measured stress tensors, left and right respectively, for these two plots are

$$\begin{bmatrix} 499 & -99 & -2 \\ -99 & 667 & -214 \\ -2 & -214 & 220 \end{bmatrix} \pm \begin{bmatrix} 150 & 34 & 36 \\ 34 & 77 & 41 \\ 36 & 41 & 107 \end{bmatrix} \quad \text{and}$$

$$\begin{bmatrix} 132 & -90 & 38 \\ -90 & 342 & -97 \\ 38 & -97 & 116 \end{bmatrix} \pm \begin{bmatrix} 132 & 31 & 31 \\ 31 & 67 & 44 \\ 31 & 44 & 76 \end{bmatrix} \text{MPa}$$

The corresponding principal stresses are

$$\begin{bmatrix} 779 & 0 & 0 \\ 0 & 438 & 0 \\ 0 & 0 & 129 \end{bmatrix} \pm \begin{bmatrix} 44 & 0 & 0 \\ 0 & 99 & 0 \\ 0 & 0 & 80 \end{bmatrix} \quad \text{and} \quad \begin{bmatrix} 412 & 0 & 0 \\ 0 & 99 & 0 \\ 0 & 0 & 80 \end{bmatrix} \pm \begin{bmatrix} 39 & 0 & 0 \\ 0 & 64 & 0 \\ 0 & 0 & 51 \end{bmatrix} \text{MPa}$$

The principal directions were always chosen on the upper half of the projection to simplify the plots. If a principal direction was computed to be on the lower half of the projection, it was replaced with its opposite direction (also a principal direction), which is on the upper half. The first plot shows a case where the principal directions are well defined. The second plot illustrates a case where the principal directions are not well determined by the data. This has two sources. First, the errors are large in comparison to the stress values and, second, two of the principal stresses are nearly equal within the experimental error. This means that there is a plane through this point where the stress components in any direction in that plane are nearly equal. This is reflected by the band in the plot representing this plane. With the experimental errors, the measurement cannot distinguish within this plane where the principal directions are.

It should be emphasized again that the directions are distributed about the original measurement's principal directions and not about the true principal directions, which are unknown. It is assumed that the distribution of directions about the true principal directions would have the same shape in the plot.

4.10 Goodness-of-fit

In Section 4.4, examining data in a $\sin^2\psi$ plot for anomalies was advocated. Knowing how the data should look will help one discover experimental difficulties. Here, we will develop a more quantifiable test that can be used to judge the quality of diffraction stress data [26].

The quantity χ^2, as defined in equation (10), gives a measure of the discrepancy between the best-fit model to the data and the actual data. For some unknown stress state being measured, an experiment will result in a value of χ^2_{obs}. This quantity is a random variable with statistical properties that can be tested to determine the quality of the fit to the data. We will use χ^2_{obs} to test the hypothesis that the data are a good fit to equation (6). If we reject this hypothesis, we must conclude that the strains computed by fitting the data to equation (6) are not a good measure of the true state of strain. This can be a result of systematic experimental errors or having a material where equation (6) does not accurately represent the state of strain for the different groups of grains giving rise to diffraction peaks for the different orientations of the diffraction vector.

χ^2_{obs} follows the χ^2 probability distribution given by [5, 17]

$$P(\chi^2, v) = \frac{(\chi^2)^{1/2(v-2)}\mathrm{e}^{-\chi^2/2}}{2^{v/2}\Gamma(v/2)} \tag{41}$$

Here v is the degrees of freedom and $\Gamma(z)$ is the gamma function. The degrees of freedom are defined as the number of observations minus the number of parameters fit. If we are fitting data to equation (6) to determine six components of strain, the degrees of freedom will be the number of strain measurements minus six. Notice that if we measure only six strains, the model will fit the data exactly and χ^2 will be exactly zero because there are no degrees of freedom left.

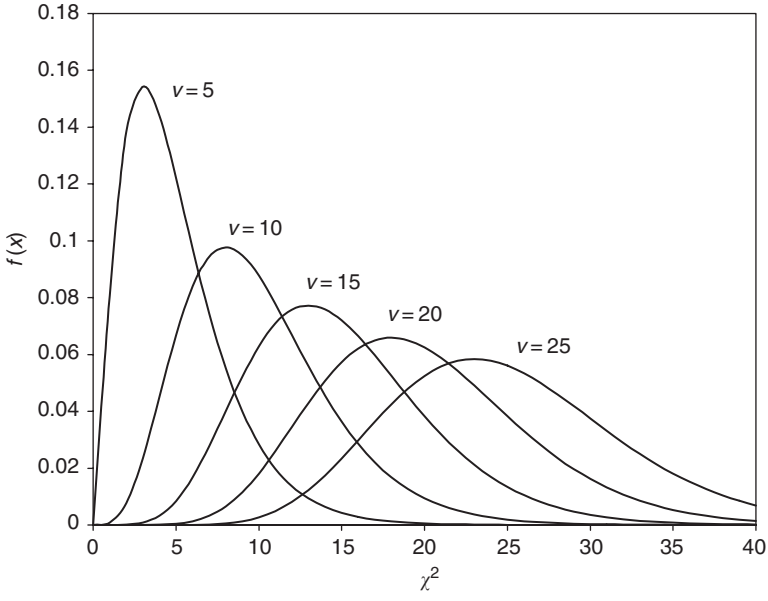

Figure 4.5 The χ^2 probability distribution for different degrees of freedom.

The χ^2 distribution for several different degrees of freedom is shown in Figure 4.5. The expected value of χ^2_{obs} is υ. Notice that as χ^2_{obs} gets larger than υ, the probability of experimentally realizing this χ^2_{obs} gets very small.

We can find the probability of experimentally realizing a χ^2 value of χ^2_{obs} or larger by integrating the probability distribution function from χ^2_{obs} to infinity. This gives the probability that a high or higher χ^2_{obs} could have occurred by random chance given our estimates of the experimental errors. We will call this probability the goodness-of-fit statistic Q, defined as

$$Q(\chi^2, \upsilon) = \int_{\chi^2}^{\infty} P(\chi^2, \upsilon) \mathrm{d}\chi^2 \tag{42}$$

We can now accept or reject the following hypothesis about a set of data:

> The model of equation (6) accurately estimates the state of strain in the sample and χ^2_{obs} is due to the estimated experimental uncertainties.

This hypothesis will be rejected if Q is too small, that is, if the probability of observing this much discrepancy between the model and the data, given the estimated uncertainties, is too low. Conversely, we accept the hypothesis when the probability Q indicates that χ^2_{obs} is likely to have occurred.

Figure 4.6 shows data from the near-surface region of a ground steel plate. Here, we observe a good fit to the data and the probability Q shows that the discrepancy between the

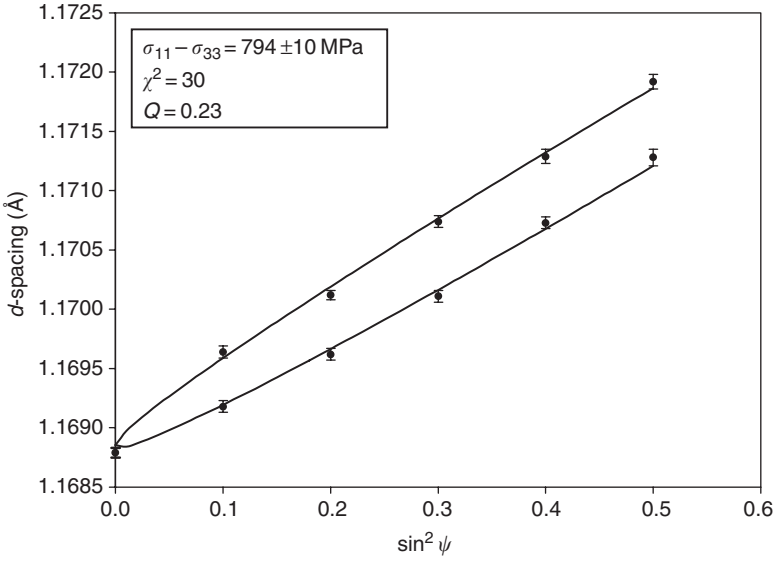

Figure 4.6 Measured d-spacings from a ground steel plate compared to the best-fit model, equation (6). This data illustrates a good fit to the strain transformation equation. The probability Q indicates that the observed variations of the data from the model are most likely due primarily to the counting errors in the measurement.

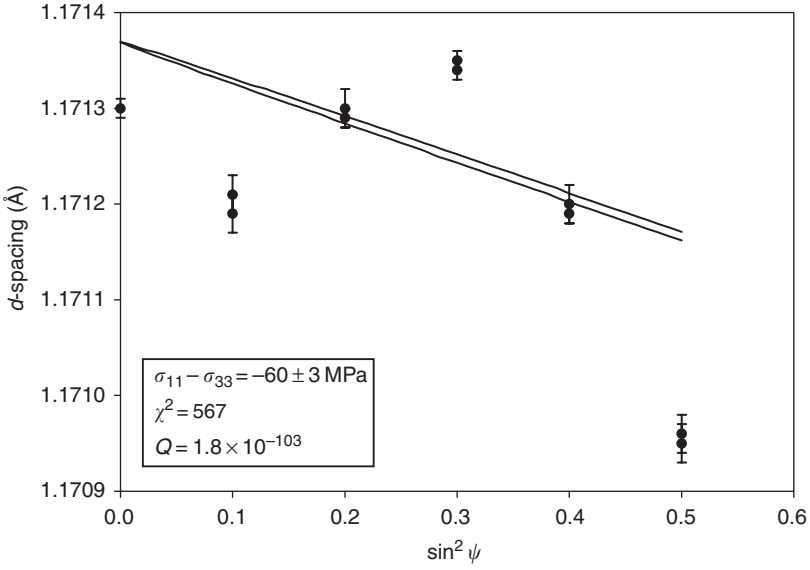

Figure 4.7 Measured d-spacings from a rolled steel plate compared to the best-fit model, equation (6). This data illustrates a poor fit to the strain transformation equation. The probability Q indicates that the data do not fit the model.

data and the model is likely to be accounted for by the estimated experimental uncertainties. In contrast, Figure 4.7 shows data from the near surface region of a cold-rolled steel sheet. This data shows oscillations with $\sin^2\psi$ that cannot be fit with the model. The extremely low probability Q gives us reason to reject our hypothesis and not accept the fitted strains as a valid measurement. Cold-rolled materials are well known to develop these oscillations due to the inhomogeneous partitioning of stress among grains of different orientations in the material. The fitting of the data to equation (6) is inappropriate, which is revealed by our goodness-of-fit test.

The following criteria have been offered for judging the quality of data with the goodness-of-fit test and accepting or rejecting the stress and strain results [26]:

$1.0 < Q < 0.01$:	Accept the hypothesis. The experimental data fits the model and the observed discrepancy is accounted for by the estimated uncertainties.
$10^{-5} < Q < 10^{-2}$:	The quality of the fit is questionable. Results may still be valid because some small experimental errors have not been accounted for. Take a closer look.
$Q < 10^{-5}$:	Reject the hypothesis. The data do not fit the model.

References

[1] Nye J. F., *Physical Properties of Crystals: Their Representation by Tensors and Matrices*, 1985, Clarendon Press, Oxford.

[2] Winholtz R. A. and Cohen J. B., *Aust. J. Phys.*, **41**, 189–199 (1988).

[3] Noyan I. C. and Cohen J. B., *Residual Stress: Measurement by Diffraction and Interpretation*, 1987, Springer-Verlag, New York.
[4] Hauk V., *Structural and Residual Stress Analysis by Nondestructive Methods*, 1997, Elsevier, Amsterdam.
[5] Press W. H., Teukolsky S. A., Vetterling W. T. and Flannery B. P., *Numerical Recipes in C: The Art of Scientific Computing*, 1992, Cambridge University Press, New York.
[6] Noyan I. C., *Metall. Trans. A*, **14A**, 1907–1914 (1983).
[7] Dölle H. and Hauk V., *Härterei-Tech. Mitt.*, **31**, 165–169 (1976).
[8] Dölle H., *J. Appl. Crystallogr.*, **12**, 489–501 (1980).
[9] Noyan I. C., *Adv. X-ray Anal.*, **28**, 281–288 (1985).
[10] Warren B. E., *X-ray Diffraction*, 1990, Dover Publications Inc., New York.
[11] Shi N., Arsenault R. J., Krawitz A. D. and Smith L. F., *Metall. Trans. A*, **24A**, 187–196 (1993).
[12] Papazian J., *Metall. Trans. A*, **19A**, 2945–2953 (1988).
[13] Dutta I. and Bourell D. L., *Mater. Sci. Eng. A*, **112**, 67–77 (1989).
[14] Krawitz A. D. and Winholtz R. A., *Mater. Sci. Eng. A*, **185**, 123–130 (1994).
[15] Winholtz R. A. and Krawitz A. D., *Mater. Sci. Eng. A*, **205**, 257–258 (1996).
[16] Winholtz R. A. and Krawitz A. D., *Mater. Sci. Eng. A*, **221**, 33–37 (1996).
[17] Bevington P. R., *Data Reduction and Error Analysis for the Physical Sciences*, 1969, McGraw-Hill, New York.
[18] Winholtz R. A. and Cohen J. B., *Mater. Sci. Eng. A*, **154**, 155–163 (1992).
[19] Winholtz R. A. and Krawitz A. D., *Proceedings of the Fifth International Congress on Residual Stresses*, 1997, Linköping, Sweden, 598–603.
[20] Winholtz R. A. and Cohen J. B., *Adv. X-ray Anal.*, **32**, 341–353 (1989).
[21] P. Karasudhi, *Foundations of Solid Mechanics*, 1991, Kluwer Academic Publishers, Dordrecht.
[22] Witte D. A., Winholtz R. A. and Neal S. P., *Adv. X-ray Anal.*, **37**, 265–278 (1994).
[23] Winholtz R. A., *J. Appl. Crystallogr.*, **28**, 590–593 (1995).
[24] Wenk H. R., in *Preferred Orientation in Deformed Metals and Rocks: An Introduction to Modern Texture Analysis*, H. R. Wenk (ed.) 1985, Academic Press, Orlando, FL, pp. 11–47.
[25] Winholtz R. A. and Krawitz A. D., *Metall. Trans. A*, **26A**, 1287–1295 (1995).
[26] Lohkamp T. A. and Winholtz R. A., *Adv. X-ray Anal.*, **39**, 281–289 (1997).